0026-895X/05/6804-966–973$20.00
MOLECULAR PHARMACOLOGY
Copyright © 2005 The American Society for Pharmacology and Experimental Therapeutics
Mol Pharmacol 68:966–973, 2005

Vol. 68, No. 4
12401/3052607
Printed in U.S.A.

Investigation of the Phenylalkylamine Binding Site in *h*Kv1.3 (H399T), a Mutant with a Reduced C-Type Inactivated State

Tobias Dreker and Stephan Grissmer

Department of Applied Physiology, University of Ulm, Ulm, Germany

Received February 28, 2005; accepted July 6, 2005

ABSTRACT

To screen for residues of *h*Kv1.3 important for current block by the phenylalkylamine verapamil, the inactivated-state-reduced H399T mutant was used as a background for mutagenesis studies. This approach was applied mainly to abolish the accumulation in the inactivated blocked state, recovery from which in the wild type is normally slow. Substitution of amino acids in the S6 transmembrane helix indicated a heavy disruption of verapamil block by the A413C mutation, reducing the IC_{50} from 2.4 to 267 μM. Subsequent scanning for verapamil moieties essential for current block was performed by application of derivatives with altered side groups. Neither the removal of the nitrile or the methyl group nor the addition of a methoxy group resulted in major variations of IC_{50} values for *h*Kv1.3 (H399T) current block. However, disruption of current block by A413C was 4- to 10-fold less pronounced for derivatives lacking the 4-methoxy group of the (3,4-dimethoxyphenyl)ethyl-methyl-amino part (devapamil) or all four methoxy groups (emopamil), respectively. Emopamil displayed a Hill coefficient of 2 for *h*Kv1.3 (H399T/A413C) instead of 1 for *h*Kv1.3 (H399T) current block. These results might indicate that the alteration of Ala413 modulates the access of phenylalkylamines to their binding site depending on the occupancy of the phenyl rings with methoxy groups. A computer-based docking model shows a subset of docked PAA conformations, with a spatial proximity between the (4-methoxyphenyl)ethyl-methyl-amino group and Ala413. The PAA binding site might therefore include a binding pocket for the aromatic ring of the ethyl-methyl-amino part in an S6–S6 interface gap.

Various small molecules have been shown to block ion fluxes through channel proteins by physically occluding the pore. In the case of the voltage-gated potassium channel Kv1.3, such structurally distinct compounds as verapamil (phenylalkylamines), WIN-17317-3 (iminodihydrochinolines), UK-78282 (benzyl piperidines), correolide (triterpenes), 4-phenyl-4-[3-(2-methoxyphenyl)-3-oxo-2-azaprop-1-yl] cyclohexanone (cyclohexyl-substituted benzamides), or Psora-4 (5-phenylalkoxypsoralens) display inhibitory effects (reviewed in Wulff et al., 2003; Vennekamp et al., 2004). An obvious possibility is to use these small molecules as probes to investigate the residues and spatial requisites of the receptor necessary for binding. Enhanced knowledge of these parameters could provide useful information for the design of more specific and potent drugs with potential therapeutic use. The phenylalkylamine (PAA) verapamil was used in this study to explore the binding site of *h*Kv1.3, a channel that plays an important role in T-cell activation and B-cell differentiation (Chandy et al., 1984; DeCoursey et al., 1984; Wulff et al., 2004). Many data have been reported already, determining the basic mode of verapamil block of Kv1.3 currents, thereby providing a good starting point for a detailed investigation of the binding pocket. Verapamil acts as a fast open-channel blocker with an IC_{50} of approximately 8 μM (Rauer and Grissmer, 1996), and block takes place from the intracellular side of the cell. Mutagenesis and competition studies suggest that the binding site is situated in the water-filled cavity below the selectivity filter (Rauer and Grissmer, 1999). The latter results might indicate that side groups of verapamil are in close contact with pore-facing residues of the transmembrane S6 helix. Hanner et al., 2001 reported that various residues in this area are important for the binding of correolides. For L-type Ca^{2+} channels, it has been shown that the PAA binding site involves residues in the S6 segments of domains III and VI (Hockerman et al., 1995, 1997; Schuster et al., 1996) and a homology model based on the KcsA channel structure has been established presenting the

This work was supported by grants from the Deutsche Forschungsgemeinschaft (GR 848/8–2) and the 4SC AG, Martinsried, Germany.

This work was presented in part as a poster [Dreker T, Lehmann-Horn F, and Grissmer S. (2005) Utilization of Kv1.3 double mutants to explore the binding site of verapamil. *Biophys J* **88:**278a].

Article, publication date, and citation information can be found at http://molpharm.aspetjournals.org.

doi:10.1124/mol.105.012401.

ABBREVIATIONS: *h*Kv1.3, human voltage-activated potassium channel; MthK, *Methanobacterium thermoautotrophicum* potassium channel; WIN-17317-3, 1-benzyl-7-chloro-4-(*n*-pentylimino)-1,4-dihydroquinoline hydrochloride; UK-78282, 4-[(diphenylmethoxy)methyl]-1-[3-(4-methoxyphenyl)propyl]-piperidine; PAA, phenylalkylamine; KTX, kaliotoxin; TEA, tetraethyl ammonium; CMV, cytomegalovirus.

PAA devapamil with the aromatic ring of the phenylethylamine part located inside the S6 interface III/IV crevice (Lipkind and Fozzard, 2003).

A specific property of Kv1.3 that distinguishes it from other Kv subfamily members is the intrinsic C-type inactivated state displayed by the channel. This state is reached slowly by all channel molecules upon depolarization, and recovery from inactivation is slow. Various drugs are known to bind selectively to the open and/or inactivated state; e.g., verapamil application leads to open blocked and inactivated blocked conformations of the channel (Röbe and Grissmer, 2000). A substantial problem of investigating drug effects on Kv1.3 currents is the difficulty to electrically distinguish between the access of the drug to either state. Upon verapamil application, one can observe an acceleration of current decay during the depolarizing steps and an accumulation of peak current block in consecutive voltage steps. The latter effect is caused by an accumulation of the channel in the inactivated blocked state, recovery from which is very slow (Röbe and Grissmer, 2000). To address this problem, we introduced the H399T mutation in the extracellular loop between the pore and the S6 helix of *h*Kv1.3, because it has been described to strongly reduce the C-type inactivated state (Nguyen et al., 1996; Rauer and Grissmer, 1996). This reduction of complexity makes the direct calculation of IC_{50} values feasible by measurement of steady-state current block. Additional amino acid substitutions in the pore-facing parts of the S6 transmembrane helix (Fig. 1) revealed that the residue at position 413 plays an important role for PAA binding. Thereafter, to detect important side groups of the ligand, block by several verapamil derivatives has been examined and the obtained results pointed out reciprocal interactions between the mutated channel residue and exchanged verapamil side groups. Double-mutant cycle analysis calculations suggested a spatial proximity between both interaction partners, information that was used to evaluate the computer based docking of a PAA molecule into an *h*Kv1.3 homology model.

Materials and Methods

Cells. The COS-7 cell line was obtained from the Deutsche Sammlung von Mikroorganismen und Zellkulturen GmbH (Braunschweig, Germany). The cells were maintained in Dulbecco's modified Eagle's medium with high glucose (Invitrogen, Carlsbad, CA) containing 10% fetal calf serum (PAA Laboratories GmbH, Coelbe, Germany) and stored in an incubator at 37°C and 10% p(CO_2).

Chemicals and Solutions. All measurements were performed in an external bath solution, high Na^+_{out} (containing 160 mM NaCl, 2 mM $CaCl_2$, 1 mM $MgCl_2$, 4.5 mM KCl, and 5 mM HEPES) or high K^+_{out} (containing 164.5 mM KCl, 2 mM $CaCl_2$, 1 mM $MgCl_2$, and 5 mM HEPES). Osmolarity was 290 to 320 mOsM, and pH was adjusted to 7.4 with NaOH or KOH, respectively. The internal pipette solution contained 155 mM KF, 2 mM $MgCl_2$, 10 mM EGTA, and 10 mM HEPES. Osmolarity was 290 to 320 mOsM, and pH was adjusted to 7.2 with KOH. All verapamil compounds were dissolved in DMSO as stock-solutions and diluted to the final concentration in external bath solution before application. DMSO fraction in the final solution was always <2%. (±)-verapamil, (−)-verapamil, (+)-verapamil, and (±)-gallopamil were obtained as hydrochloride salts from Sigma-Aldrich (St. Louis, MO). (−)-devapamil (LU 47093), (±)-norverapamil (LU 41723) and (±)-acyanoverapamil (LU 44935) were provided as hydrochloride salts by Drs. Raschack and Paul of Knoll Pharmaceuticals AG (now merged in Abbott GmbH and Co. KG (Ludwigshafen, Germany). (±)-emopamil (LU 37076) was a generous gift from Dr. Hans-Günther Knaus and Dr. Hartmut Glossmann (Institut für Biochemische Pharmakologie, Medizinische Universität Innsbruck, Innsbruck, Austria). KTX (Latoxan, Valence, France; Bachem, Bubendorf, Switzerland) was dissolved in external bath solution containing 0.1% bovine albumin (Sigma-Aldrich). TEA chloride was purchased from Fluka (Buchs, Switzerland) and dissolved in external bath solution to the respective final concentration.

Electrophysiology. The whole-cell recording mode of the patch-clamp technique (Hamill et al., 1981) was used throughout all measurements. Experiments were carried out at room temperature (18–22°C), and external bath solution and diluted drug solutions were applied using a gravity-based permanent perfusion system. Electrodes were pulled from glass capillaries (Science Products, Hofheim, Germany) in three stages and fire-polished to resistances of 2 to 4 MΩ. Data were acquired with an EPC-9 patch-clamp amplifier (HEKA Elektronik, Lambrecht/Pfalz, Germany) connected to a Macintosh computer running Pulse/Pulse Fit ver. 8.40 data acquisition and analysis software (HEKA). All currents were filtered by a 2.9-kHz Bessel filter and recorded with a sampling frequency of 2.00 kHz. Capacitative and leak currents were subtracted, and series resistance compensation (80%) was used for currents exceeding 2 nA. Further data analysis was performed using the Igor Pro 3.1 (Wavemetrics, Lake Oswego, OR) software package. Holding potential was usually −80 mV (*h*Kv1.3 mutants) or −120 mV (*h*Kv1.3 wild type). Time constants τ_m and τ_h and steady-state currents with and without drug application were determined by a Hodgkin and Huxley fit to currents elicited by a 200-ms voltage pulse from the holding potential to +40 mV. The deactivation time constant τ_t was obtained by an exponential fit to tail currents at −60 mV observed after a voltage pulse from the holding potential to +40 mV for 200 ms. Parameters $V_{1/2}$ and k were deduced from a Boltzmann fit to either normalized maximum peak conductance elicited by 11 consecutive voltage steps from −50 to +50 mV (ΔV = 10 mV) in high Na^+_{out} or to maximum tail peak currents at −80 mV after the voltage steps in high K^+_{out}. Drug effects were evaluated by the steady-state current block obtained during 200-ms voltage steps from the holding potential to +40 mV. Time interval between pulses was 30 s, allowing the channel to recover from inactivation completely. IC_{50} values were calculated by fitting a Hill function ($I_{drug}/I_0 = 1/[1+(IC_{50}/C_{drug})^{nH}]$) to the normalized steady-state current data points obtained after drug application. I_0 represents the steady state current before and I_{drug} the steady state current after drug application, C_{drug} the concentration of the drug in the external bath solution and n_H the Hill coefficient.

Molecular Biology. The *h*Kv1.3 wild-type plasmid was a generous gift from Prof. Dr. O. Pongs (Institut für Neurale Signalverarbeitung, Zentrum für Molekulare Neurobiologie, Hamburg, Germany). It contains the *human* Kv1.3 K^+ channel gene in a pRc/CMV vector (Invitrogen) with a CMV promoter for protein expression in

```
  71 LGMYFTVTLIVLGIGTFAVAVERLLEF MthK
  87 WGRLVAVVVMVAGITSFGLVTAALATW KcsA
 454 WGKIVGSLCAIAGVLTIALPVPVIVSN Shaker
 404 GGKIVGSLCAIAGVLTIALPVPVIVSN Kv1.3
1143 VEISIFFIIYIIIIAFFMMNIFVGFVI L-type Ca2+ III S6
1454 FAVFYFISFYMLCAFLIINLFVAVIMD L-type Ca2+ IV S6
```

Fig. 1. Alignment of the S6 domains of several ion channels. The mutated amino acids in *h*Kv1.3 are highlighted as white letters with a black background; the residues in L-type Ca^{2+} channels important for PAA block are indicated by a gray background. The presumed gating hinge glycine of the K^+ channels is outlined by a frame.

mammalian cells. Channel mutants were generated by introducing the corresponding point mutations in the cloned *h*Kv1.3 gene with the QuikChange site-directed mutagenesis kit (Stratagene, La Jolla, CA). Transfection of COS-7 cells was done using the Fugene 6 transfection reagent (Roche Molecular Biochemicals, Mannheim, Germany). Cells were grown to ~80% confluence and cotransfected with ~1 μg of *h*Kv1.3 DNA and ~0.5 μg of eGFP-N1 DNA (BD Biosciences Clontech, Palo Alto, CA). One day after transfection sufficient protein for electrophysiological measurements was expressed.

Double Mutant Cycle Analysis. The coupling coefficient Ω was calculated by the equation $\Omega = [IC_{50}(R_{wt}, L_{wt}) \times IC_{50}(R_{mt}, L_{mt})]/[IC_{50}(R_{wt}, L_{mt}) \times IC_{50}(R_{mt}, L_{wt})]$, according to Hidalgo and MacKinnon (1995). R_{wt} was the receptor "wild type" *h*Kv1.3 (H399T) and R_{mt} was the H399T/A413C double mutant. L_{wt} represents the "wild-type" drug [(±)-verapamil or (−)-verapamil] and L_{mt} represents the "mutant" drug (a verapamil derivative with an exchanged side group). If coupling coefficients of less than 0 were obtained, the reciprocal value was taken. The change of free binding energy ($\Delta\Delta G$) was calculated by the equation $\Delta\Delta G = RT\ln\Omega$, where R is the gas constant and T is absolute temperature.

Results

***h*Kv1.3 (H399T) As a Tool for Determination of Steady State PAA Block.** To minimize the time the channel spends in the C-type inactivated state of *h*Kv1.3, the H399T mutation, which is analogous to the H404T mutation in *m*Kv1.3, was introduced (Nguyen et al., 1996; Rauer and Grissmer, 1996). Figure 2 shows the K^+ currents through *h*Kv1.3 wild type (A) and H399T mutant (B) channels, without drug application (pulse 1). The inactivation time constant (τ_h) of *h*Kv1.3 (H399T) is approximately 2.3-fold slower compared with wild type (Fig. 2; Table 1), and investigation of the kinetics for recovery from inactivation (Fig. 3, A and B) revealed that the corresponding time constant τ_{rec} of *h*Kv1.3 H399T is approximately 10 times faster (Table 1) than in case of the wild type. The intrinsic activation parameters ($V_{1/2}$, k, and τ_m) of *h*Kv1.3 (H399T) are similar to the corresponding wild-type values, whereas the deactivation time constant τ_t at −60 mV is increased by a factor of approximately 3.7 (Table 1). Application of 20 μM (±)-verapamil resulted in a steady-state block of *h*Kv1.3 (H399T) currents at the end of a 200-ms pulse and no further accumulation of peak current block in consecutive pulses (Fig. 2B, pulse 2–4). The normalized steady-state current after PAA application should therefore directly reflect the ratio of channels in the open blocked and open states. The remaining inactivation of the mutant *h*Kv1.3 channels after 200 ms was ignored for the evaluation of steady-state block.

Identification of *h*Kv1.3 (H399T) Residues Important for PAA Block. Several amino acids in the S6 transmembrane helix of *h*Kv1.3 (H399T) have been substituted, because effects of these residues on current block by verapamil or similar drugs to Kv1.3 or other ion channels have been described or assumed. Substitutions were performed mainly with cysteines to allow a chemical modification in future experiments. Exceptions were the H399T/S410G and H399T/G416A double mutants. In the first case, the corresponding glycine of Kv2.1 was introduced; in the second case, an alanine was introduced because of the critical function of Gly416 as the potential gating hinge (Jiang et al., 2002b). The obtained double mutants, H399T/S410G, H399T/C412A, H399T/L418C, and H399T/I420C, had only minor or moderate effects on (±)-verapamil block (data not shown). The H399T/G416A mutation resulted in no functional expression of channel protein, possibly because of the disruption of the gating hinge. Another double mutant, H399T/A413C, displayed an affinity for (±)-verapamil that was reduced by a factor of approximately 100 (Table 2) compared with *h*Kv1.3 (H399T). Steady-state current block with no further accumu-

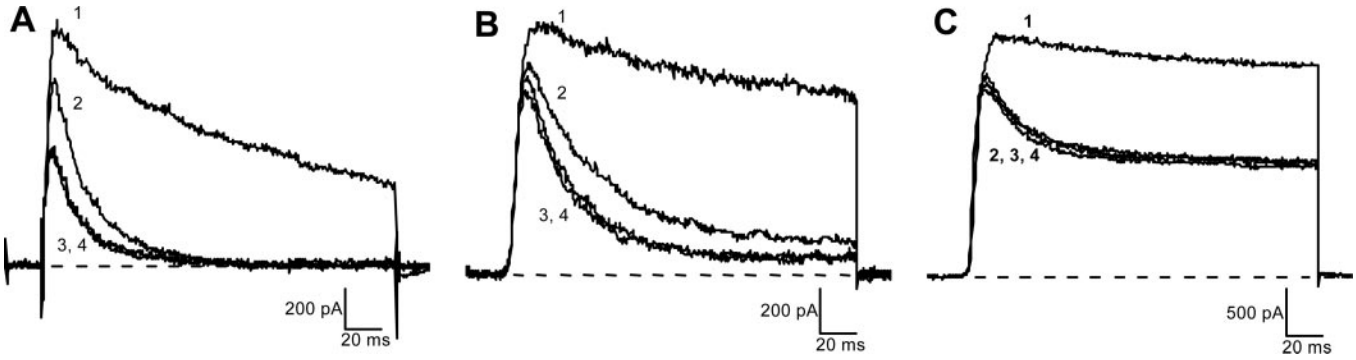

Fig. 2. K^+ currents through *h*Kv1.3 wild-type and mutant channels before and after verapamil application. A, *h*Kv1.3 wild type, 20 μM verapamil application after pulse 1. B, *h*Kv1.3 (H399T), 20 μM verapamil application after pulse 1. C, *h*Kv1.3 (H399T/A413C), 200 μM verapamil application after pulse 1. Currents were elicited by a 200-ms voltage pulse to +40 mV every 30 s.

TABLE 1
Intrinsic properties of *h*Kv1.3 wild type and mutants in transiently transfected COS-7 cells
All values are given as mean ± S.D.; numbers of independent experiments are given in parentheses.

	*h*Kv1.3		
	Wild Type	H399T	A413C/H399T
$V_{1/2}$ (mV)	−33 ± 1 (2)	−36 ± 1 (9)	−37 ± 1 (3)
k (mV)	10 ± 1 (2)	7 ± 1 (9)	7 ± 1 (3)
τ_m (ms)	2.9 ± 0.4 (6)	3.9 ± 0.7 (10)	4.9 ± 1.1 (10)
τ_h at 40 mV (ms)	291 ± 53 (6)	678 ± 134 (10)	1220 ± 200 (10)
τ_t at −60 mV (ms)	117 (1)	434 ± 119 (8)	30 ± 14 (9)
τ_{rec} at −120 mV (s)	13.6 ± 0.2 (4)	≤ 1.1 (4)	≤ 1.1 (4)

lation of block could still be observed in this channel mutant (Fig. 2C, pulses 2–4). Furthermore, *h*Kv1.3 (H399T/A413C) exhibits an even slower intrinsic inactivation rate (~2-fold), a similar recovery from inactivation (Fig. 3C; Table 1), and an accelerated deactivation rate (~10-fold) compared with *h*Kv1.3 (H399T) (Fig. 2C, pulse 1; Table 1). The activation parameters ($V_{1/2}$, k, τ_m) also remain similar.

Current Block by Externally Applied KTX and TEA Is Affected by Introduction of A413C in *h*Kv1.3 (H399T). Effects on the affinity for externally applied KTX and TEA have been examined to investigate whether the introduced cysteine decreases the affinity for (±)-verapamil merely by a direct interaction with the drug or by allosteric changes of the three dimensional protein structure. Both inhibitors are known to bind to the extracellular vestibule of Kv1.3 (Kavanaugh et al., 1991; Wrisch and Grissmer, 2000) and could serve as probes for structural differences in the extracellular region of the double mutant. In the case of *h*Kv1.3 (H399T), IC_{50} values of 25.9 ± 2.5 mM for TEA and 0.25 ± 0.02 nM for KTX (Fig. 4, A and B, filled bars) were obtained. IC_{50} values for KTX and TEA block differed for *h*Kv1.3 (H399T/A413C), with 5.8 ± 0.4 mM for TEA and 0.66 ± 0.06 nM for KTX (Fig. 4, A and B, open bars).

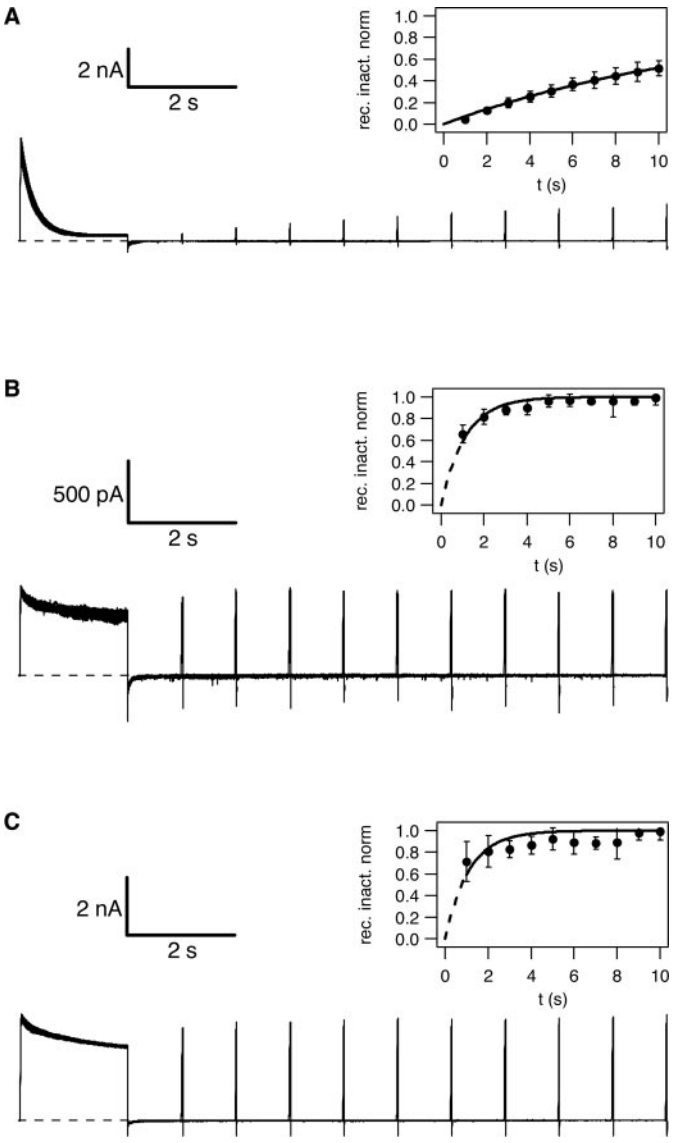

Fig. 3. Recovery from inactivation of *h*Kv1.3 wild type (A), *h*Kv1.3 (H399T) (B), and *h*Kv1.3 (H399T/A413C) (C) channels. Currents were elicited by double-pulse protocols, with a 2-s conditioning pulse and a 30-ms test pulse to +40 mV, after different repolarization times to −120 mV from 1 to 10 s. The resulting currents are displayed as superimposed traces. The inserts show the normalized recovery from inactivation, with the data points calculated from the difference of the peak current of the test pulse and the steady-state current of the conditioning pulse divided by the difference of the peak current and the steady-state current of the conditioning pulse. Fits were performed by a monoexponential function yielding a time constant τ_{rec} of 13.6 s for wild-type *h*Kv1.3 (A). Time constants for *h*Kv1.3 (H399T) (B) and *h*Kv1.3 (H399T/A413C) (C) were estimated to be ≤1.1 s due to 65 and 71% recovery from inactivation after 1 s of repolarization, respectively (Table 1).

Importance of A413 for the Stereoselectivity of Verapamil Block. Verapamil is a chiral compound and current block by both enantiomers was investigated. These experiments were necessary for comparison with current block by (−)-devapamil and to select the appropriate enantiomer for subsequent docking computations. (−)-Verapamil blocked *h*Kv1.3 (H399T) currents with an approximately 3.6-fold higher potency compared with the (+)-enantiomer (Table 2). It is surprising that the introduced A413C mutation reduced the affinity for (−)-verapamil by a factor of ~200, whereas the affinity for (+)-verapamil was reduced by a factor of ~80 only (Table 2). Thus, the ability of the channel to discriminate between both enantiomers seems to be almost lost in the double mutant, leaving a preference of 1.4-fold for (−)-verapamil over (+)-verapamil.

Inhibition Properties among Distinct Verapamil Derivatives Are Different for *h*Kv1.3 (H399T) and *h*Kv1.3 (H399T/A413C). Verapamil contains various functional groups, each of which might or might not play an important role in blocking Kv1.3 currents. For this reason, block of currents through *h*Kv1.3 (H399T) and the double mutant H399T/A413C by several verapamil derivatives (Fig. 5) was investigated. Compared with (±)-verapamil, the compounds (±)-emopamil, (±)-gallopamil, (±)-norverapamil, and (±)-acyanoverapamil displayed only subtle variations in the IC_{50} values for *h*Kv1.3 (H399T) current block. The same result was obtained for the (−)-verapamil compared with the (−)-devapamil IC_{50} value. However, in case of the *h*Kv1.3 (H399T/A413C) double mutant, the results were partially different. Whereas (±)-gallopamil, (±)-norverapamil, and (±)-acyanoverapamil IC_{50} values are still similar to that of (±)-verapamil, (±)-emopamil block is approximately 10 times less affected by the A413C mutation. Another remarkable finding was that (±)-emopamil block of *h*Kv1.3 (H399T/A413C) currents was the only case in which the dose-re-

TABLE 2

IC_{50} values for steady state PAA block of *h*Kv1.3 (H399T) and *h*Kv1.3 (H399T/A413C) currents

All values were obtained from at least four independent experiments and are given as mean ± S.D.

PAA	*h*Kv1.3 (H399T)	*h*Kv1.3 (A413C/H399T)
	μM	
(±)-Verapamil	2.4 ± 0.2	267 ± 22
(−)-Verapamil	1.2 ± 0.2	258 ± 24
(+)-Verapamil	4.3 ± 0.5	356 ± 47
(−)-Devapamil	0.7 ± 0.1	66 ± 8
(±)-Emopamil	2.0 ± 0.2	25 ± 2[a]
(±)-Gallopamil	3.4 ± 0.4	314 ± 29
(±)-Norverapamil	1.5 ± 0.3	228 ± 25
(±)-Acyanoverapamil	1.9 ± 0.2	246 ± 34

[a] Hill coefficient = 2.

sponse fits resulted in a Hill coefficient of 2 instead of 1 (Fig. 6). Comparison of (−)-devapamil and (−)-verapamil IC_{50} values for the double mutant also suggests a smaller influence of A413C on (−)-devapamil current block, which is 4-fold more potent compared with (−)-verapamil.

Double Mutant Cycle Analysis of the Obtained IC_{50} Values. To detect coupled interactions caused by the substitution of the alanine at position 413 and the alteration of the different side groups of verapamil, the coupling coefficients (Ω) and the change of free binding energies (ΔΔG) were calculated for all reactions (Table 3). In this approach, interdependency between two interaction partners is indicated by Ω values deviating from 1. Whereas the coupling coefficients calculated for gallopamil, norverapamil, and acyanoverapamil stayed near 1, Ω calculated for the (−)-verapamil/(−)-devapamil pair was 2.5, and the corresponding change of free binding energy was 0.52 kcal/mol. These data suggest a mutual influence of the deletion of the R_2' methoxy group of verapamil and the substitution of A413 of *h*Kv1.3 (H399T). Furthermore, an interpretation of the correlations made by Schreiber and Fersht, 1995 suggests that a change in free binding energy of >0.5 kcal/mol might indicate a spatial distance between both interaction partners of less than 5 Å.

Building an *h*Kv1.3 Homology Model and Docking of a PAA. To accommodate the inability of verapamil to bind to the closed conformation of Kv1.3 (DeCoursey, 1995), a suitable model for a K^+ channel in the open state had to be selected. The X-ray structure of MthK, a Ca^{2+} gated K^+ channel in the open conformation (Jiang et al., 2002a), was chosen as a scaffold for the homology model of *h*Kv1.3. The *h*Kv1.3 primary sequence from positions 352 to 431 was aligned to MthK, covering the S5 and S6 transmembrane helices and the pore region (Deep View software package; Guex and Peitsch, 1997). Thereafter, the *h*Kv1.3 homology model was calculated using the SWISS-MODEL server (Peitsch, 1995; Guex and Peitsch, 1997; Schwede et al., 2003). Finally, docking was performed with the AutoDock 3.0 software package (Goodsell and Olson, 1990; Morris et al., 1996, 1998) using a modified (−)-verapamil molecule as a ligand. This molecule lacks the R_4 nitrile and R_5 methyl groups, because these side groups did not show an important effect on current block in either the H399T or the A413C/H399T mutant. Of 256 docked conformations obtained, only those 31 were selected with the C atom of the R_2' methoxy group situated less than 5 Å away from the C atom of one of the four A413 side chains. No strength of interaction was implicated. Despite the symmetrical nature of the channel model, 24 methoxy groups were in proximity to Ala413 from a single subunit (Fig. 7, cyan). Within this group, two populations of similar conformations could be identified: cluster I (Fig. 7, magenta), which consisted of 12 PAAs situated in a stretched conformation in the inner vestibule of the channel with their R_1',R_2'-dimethoxyphenyl rings inserted slightly between two S6 helices, and cluster II (Fig. 7, gray), which contained four molecules in a similar stretched configuration but with their R_1',R_2'-dimethoxyphenyl rings extended deeper into the S6 interface crevice.

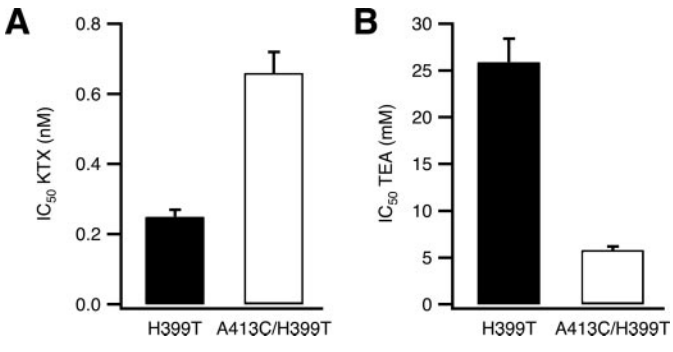

Fig. 4. Comparison of IC_{50} values for steady-state current block by external TEA and KTX for *h*Kv1.3 (H399T) and *h*Kv1.3 (H399T/A413C). All values were obtained from at least four independent experiments and are given as mean ± S.D.

Discussion

The purpose of this study was to characterize the binding site of verapamil in the *h*Kv1.3 mutant H399T, a channel mutant with a reduced C-type inactivated state. Mutations of residues in the S6 domain and application of different verapamil derivatives revealed interdependencies between position 413 of the channel and functional groups of verapamil. This information was used to deduce a more detailed description of the binding pocket.

As anticipated, the introduced H399T mutation reduced the channel's C-type inactivation but not to the extent described for an analogous *m*Kv1.3 (H404T) mutant (Rauer and Grissmer, 1996). Nonetheless, *h*Kv1.3 (H399T) was selected as a Kv1.3 model channel with a strongly reduced C-type inactivated state because the time constant for recovery from inactivation was approximately 10-fold faster compared with the wild-type channel. Steady-state currents were clearly observable with or without drug application after 1 s (data not shown) voltage pulses to +40 mV and no accumulation of steady-state current block in consecutive pulses was present.

Subsequent substitutions of amino acids in the S6 domain of *h*Kv1.3 (H399T) pointed out that the residue at position 413 plays an important role in PAA binding. By exchanging the alanine at position 413 for a cysteine, (±)-verapamil affinity was decreased by approximately 100-fold. Similar results were obtained by Hanner et al. (2001) for an *h*Kv1.3 (A413C) mutant that displayed a

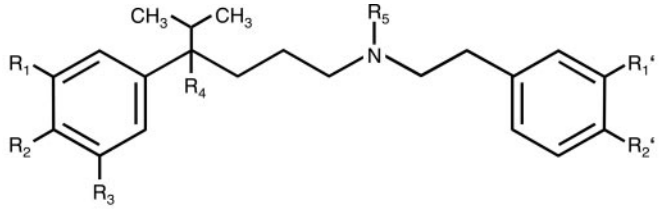

	R_1, R_1'	R_2	R_2'	R_3	R_4	R_5
verapamil	OCH_3	OCH_3	OCH_3	H	CN	CH_3
devapamil	OCH_3	OCH_3	H	H	CN	CH_3
emopamil	H	H	H	H	CN	CH_3
gallopamil	OCH_3	OCH_3	OCH_3	OCH_3	CN	CH_3
norverapamil	OCH_3	OCH_3	OCH_3	H	CN	H
acyanoverapamil	OCH_3	OCH_3	OCH_3	H	H	CH_3

Fig. 5. Chemical structures of verapamil and verapamil derivatives.

40-fold lower affinity for diTC binding compared with the wild type. Furthermore, the corresponding residue in IVS6 of L-type Ca^{2+} channels had a strong influence on PAA affinity (Hockerman et al., 1995).

The additional A413C mutation slowed the C-type inactivation rate even further, an effect that had also been observed for the *h*Kv1.3 (A413C) single mutant (data not shown). More evidence for A413 playing a role in the inactivation process was found by Panyi et al. (1995), where a strong increase of the inactivation rate in an *h*Kv1.3 (A413V) mutant was described.

It has been reported that binding of external TEA slowed C-type inactivation (Grissmer and Cahalan, 1989; Choi et al., 1991) and that the transition to the inactivated state induced structural changes in the outer pore region (Yellen et al., 1994; Liu et al., 1996; Kiss et al., 1999). Further disruption of the inactivation process by introduction of A413C might therefore explain the affinity shift observed for TEA. However, no correlations between KTX binding and C-type inactivation have been described yet. The ~3-fold decrease of KTX and 5-fold increase of TEA affinity in *h*Kv1.3 (H399T/A413C) might be due to a structural rearrangement of the channel protein in the double mutant that affects the extracellular vestibule. This rearrangement might change the intracellular vestibule as well, which could explain the dramatic decrease in verapamil affinity.

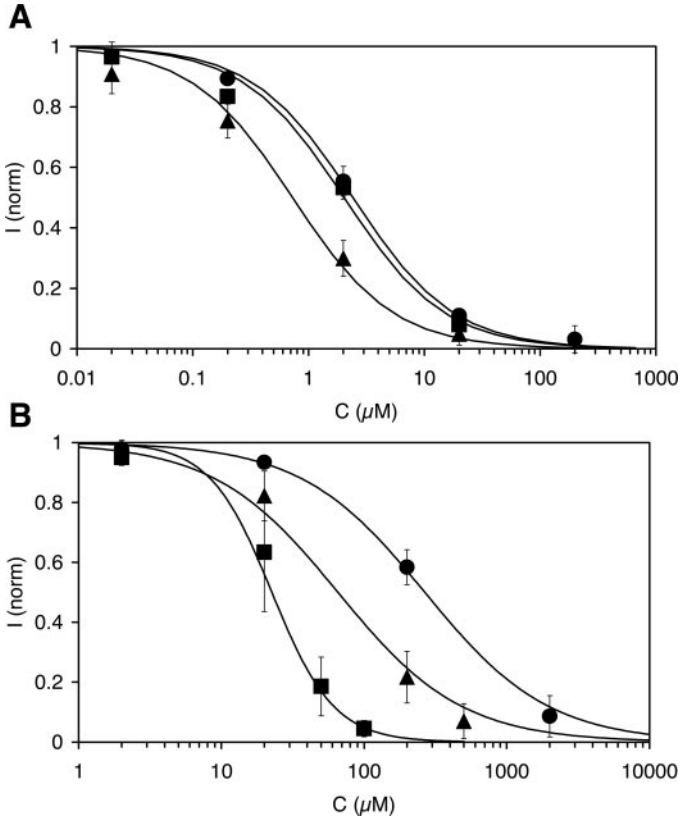

Fig. 6. Dose-response curves for block of *h*Kv1.3 (H399T) (A) and *h*Kv1.3 (A413/H399T) (B) steady-state currents by (±)-verapamil (●) and by the verapamil derivatives (−)-devapamil (▲) and (±)-emopamil (■). Hill coefficients of all fits were 1, except for (±)-emopamil block of *h*Kv1.3 (A413/H399T) currents (B, ■), in which case the Hill coefficient was 2. All data points were obtained from at least four independent experiments and are given as mean ± S.D.

Another explanation for the disruption of PAA block might be the loss of direct effects of the residue at position 413 on binding of distinct verapamil side groups. Verapamil derivatives lacking the methyl group at R_5 (norverapamil) or the nitrile group at R_4 (acyanoverapamil) did not show major variations in *h*Kv1.3 (H399T) and *h*Kv1.3 (H399T/A413C) current block compared with (±)-verapamil. Thus, neither the R_5 methyl group nor the R_4 nitrile group seems to play an important role for PAA binding in both channel mutants. The importance of the four methoxy groups at the R_1, R_1' and R_2, R_2' positions of both phenyl rings was assessed by investigation of (±)-emopamil block, a verapamil derivative that lacks all four moieties. In case of *h*Kv1.3 (H399T) only little difference could be observed between the affinities for (±)-verapamil and (±)-emopamil, suggesting no major relevance of the methoxy groups. However, as an inhibitor of *h*Kv1.3 (H399T/A413C) currents, (±)-emopamil is an approximately 10-fold more potent than (±)-verapamil. In addition, fits of the corresponding (±)-emopamil dose-response curve indicated a 2:1 ligand/receptor stoichiometry. So far, the binding of two small molecule inhibitors to *h*Kv1.3 has been demonstrated only for disubstituted cyclohexyl compounds (Schmalhofer et al., 2002, 2003) and 5-phenylalkoxypsoralens (Vennekamp et al., 2004). To investigate the importance of the methoxy groups in more detail, we examined the effects of (±)-gallopamil, which has an additional methoxy group at R_3, and (−)-devapamil, that lacks the methoxy group at R_2'. Although the R_3 methoxy group seems to have little influence on block of *h*Kv1.3 (H399T) and *h*Kv1.3 (H399T/A413C) currents, the missing R_2' methoxy group increases apparent inhibition 4-fold in the double mutant only. This effect is weaker but similar to the one obtained by removal of all four methoxy groups. However, the Hill coefficient for (−)-devapamil block of *h*Kv1.3 (H399T/A413C) currents remains at 1. Johnson et al. (1996) demonstrated that in wild-type Ca^{2+} channels, (−)-devapamil inhibits currents much more strongly than verapamil, whereas in the Y1463F mutant, this preference is lost. This mutation seems to have the opposite effect on

TABLE 3

Coupling coefficients (Ω) and change of free binding energies (ΔΔG) calculated by double mutant cycle analysis of the IC_{50} values for *h*Kv1.3 (H399T) and *h*Kv1.3 (H399T/A413C) current block by verapamil and verapamil derivatives

Wild Type Drug	Mutant Drug	Coupling Coefficient Ω	ΔΔG
			kcal/mol
(−)-Verapamil	(−)-Devapamil	2.46 ± 0.61	0.52 ± 0.15
(±)-Verapamil	(±)-Gallopamil	1.18 ± 0.21	0.09 ± 0.10
(±)-Verapamil	(±)-Emopamil	9.00 ± 1.51	1.28 ± 0.10
(±)-Verapamil	(±)-Norverapamil	1.39 ± 0.34	0.19 ± 0.14
(±)-Verapamil	(±)-Acyanoverapamil	1.20 ± 0.24	0.11 ± 0.12

PAA binding compared with A413C in *h*Kv1.3 (H399T). It is striking that the removal of a single hydroxyl group in Y1463F was responsible for the affinity changes, whereas a single thiol group was added by the A413C mutation.

The missing R_2' methoxy group of (−)-devapamil accounts solely for the altered affinity to *h*Kv1.3 (H399T/A413C) compared with (−)-verapamil. This might indicate coupled effects of the removal of the R_2' OCH_3 group and the substitution at position 413. The double mutant cycle analysis results support this line of argument, suggesting a distance of less than 5 Å between both interaction partners.

The assignment of this spatial constriction to the *h*Kv1.3/PAA docking results yielded two clusters of PAA molecules with the R_1', R_2'-dimethoxyphenyl ring located at the entrance (cluster I) or the core (cluster II) of an S6–S6 interface gap. These results are similar to those obtained by Lipkind and Fozzard (2003) for a detailed PAA docking model for an L-type Ca^{2+} channel.

Figure 8 represents a possible explanation for the observed effects. If the permeation of the ethyl-methyl-aminophenyl ring into the S6 interface crevice is an essential mechanism of PAA binding (Fig. 8A), it might be sterically constricted by introduction of the A413C mutation (Fig. 8B). However, the degree of constriction seems to be less pronounced with a decreasing number of methoxy groups present at the ethyl-methyl-aminophenyl ring. In addition, the introduction of A413C enables emopamil, which lacks all four methoxy groups at both phenyl rings, to bind with a 2:1 stoichiometry (Fig. 8B, right). The altered PAA binding pocket might therefore implicate a constricted access and a spatial dilation that allows a second PAA to bind to the channel, if the first is able to enter deeply into the S6 interface gap.

Summary. Screening of the inactivated state reduced *h*Kv1.3 (H399T) channel for residues participating in verapamil block revealed an important influence of the residue at position 413 in the S6 domain. Further inhibition experiments with verapamil derivatives suggest interdependence between the number of methoxy substituents at the PAA phenyl rings and alterations of Ala413. These data, taken together with information obtained by a computer-based docking model, might indicate that residue 413 is important for access of the PAA ethyl-methyl-aminophenyl ring to a binding pocket in an S6 interface gap.

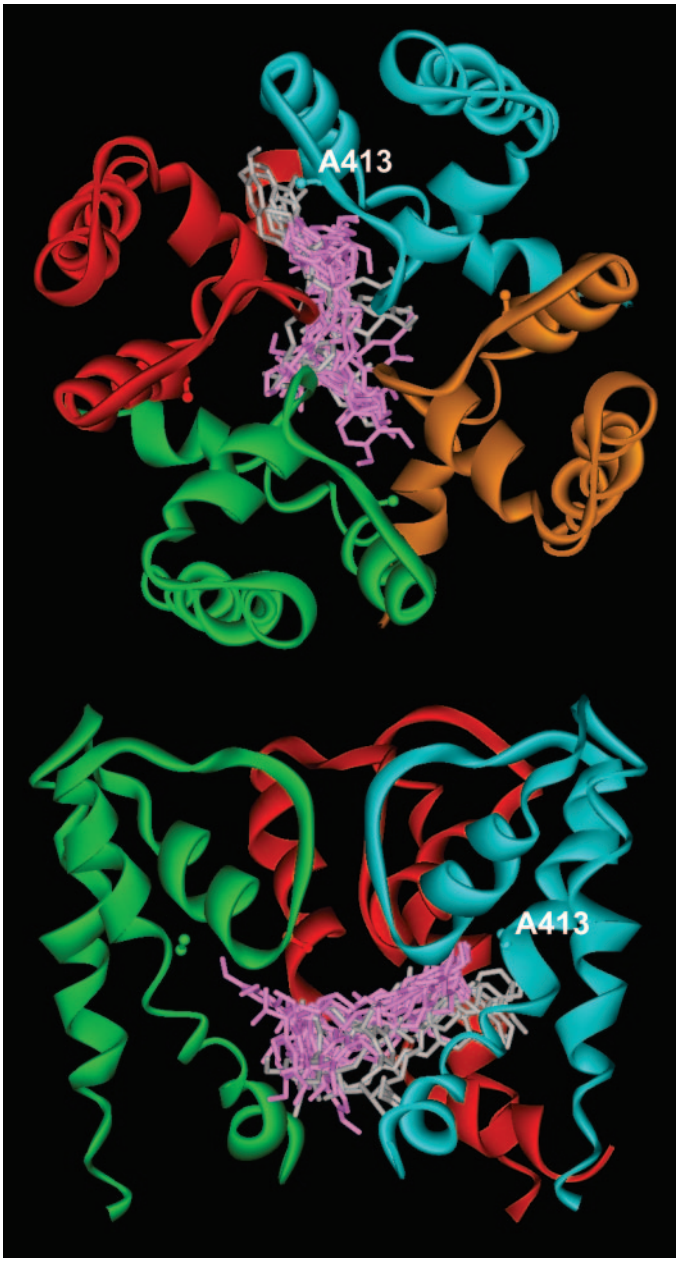

Fig. 7. Modified (−)-verapamil structure without the R_4 nitrile and the R_5 methyl group docked into a *h*Kv1.3/MthK homology model (subunits are drawn in cyan, orange, green, and red, respectively). Axial view from the extracellular side through the pore (top) and lateral view with the extracellular part oriented upward and one subunit omitted (bottom). Within the docked conformations, with the R_2'-methoxy group being in proximity to Ala413 (drawn in 'ball and stick' representation), two populations could be identified. Cluster I (magenta, 12 structures) with the phenyl ring entering slightly into an S6–S6 interface crevice and cluster II (gray, four structures) with the phenyl ring inserting deeply between both S6 helices of the red and cyan subunit. Images were generated using the ViewerLite 5.0 software package (Accelrys, San Diego, CA).

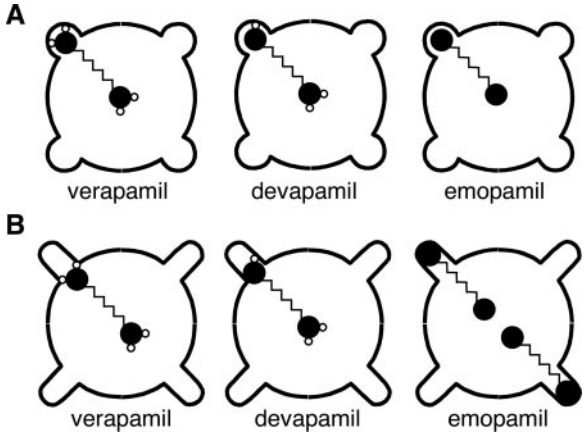

Fig. 8. Hypothetical schematic model explaining the binding of verapamil (left) and the verapamil derivatives devapamil (middle) and emopamil (right) to *h*Kv1.3 (H399T) (A) and *h*Kv1.3 (H399T/A413C) (B), respectively. The black outlines represent a cross-section through the inner vestibule of the channel, with the binding pocket of each subunit for a PAA phenyl ring marked as a bulge. These binding pockets might be altered in *h*Kv1.3 (H399T/A413C) because of the introduction of the cysteine. The PAAs are displayed in a simplified fashion as two connected black circles representing the phenyl rings with small empty circles indicating the sterical differences determined by the methoxy groups.

References

Chandy KG, DeCoursey TE, Cahalan MD, McLaughlin C, and Gupta S (1984) Voltage-gated potassium channels are required for human T lymphocyte activation. *J Exp Med* **160:**369–385.

Choi KL, Aldrich RW, and Yellen G (1991) Tetraethylammonium blockade distinguishes two inactivation mechanisms in voltage-activated K^+ channels. *Proc Natl Acad Sci USA* **88:**5092–5095.

DeCoursey TE (1995) Mechanism of K^+ channel block by verapamil and related compounds in rat alveolar epithelial cells. *J Gen Physiol* **106:**745–779.

DeCoursey TE, Chandy KG, Gupta S, and Cahalan MD (1984) Voltage-gated K^+ channels in human T lymphocytes: a role in mitogenesis? *Nature (Lond)* **307:**465–468.

Goodsell DS and Olson AJ (1990) Automated docking of substrates to proteins by simulated annealing. *Proteins* **8:**195–202.

Grissmer S and Cahalan M (1989) TEA prevents inactivation while blocking open K^+ channels in human T lymphocytes. *Biophys J* **55:**203–206.

Guex N and Peitsch MC (1997) SWISS-MODEL and the Swiss-PdbViewer: an environment for comparative protein modeling. *Electrophoresis* **18:**2714–2723.

Hamill OP, Marty A, Neher E, Sakmann B, and Sigworth FJ (1981) Improved patch-clamp techniques for high-resolution current recording from cells and cell-free membrane patches. *Pflueg Arch Eur J Physiol* **391:**85–100.

Hanner M, Green B, Gao YD, Schmalhofer WA, Matyskiela M, Durand DJ, Felix JP, Linde AR, Bordallo C, Kaczorowski GJ, et al. (2001) Binding of correolide to the K(v)1.3 potassium channel: characterization of the binding domain by site-directed mutagenesis. *Biochemistry* **40:**11687–11697.

Hidalgo P and MacKinnon R (1995) Revealing the architecture of a K^+ channel pore through mutant cycles with a peptide inhibitor. *Science (Wash DC)* **268:**307–310.

Hockerman GH, Johnson BD, Abbott MR, Scheuer T, and Catterall WA (1997) Molecular determinants of high affinity phenylalkylamine block of L-type calcium channels in transmembrane segment IIIS6 and the pore region of the alpha1 subunit. *J Biol Chem* **272:**18759–18765.

Hockerman GH, Johnson BD, Scheuer T, and Catterall WA (1995) Molecular determinants of high-affinity phenylalkylamine block of L-type calcium channels. *J Biol Chem* **270:**22119–22122.

Jiang Y, Lee A, Chen J, Cadene M, Chait BT, and MacKinnon R (2002a) Crystal structure and mechanism of a calcium-gated potassium channel. *Nature (Lond)* **417:**515–522.

Jiang Y, Lee A, Chen J, Cadene M, Chait BT, and MacKinnon R (2002b) The open pore conformation of potassium channels. *Nature (Lond)* **417:**523–526.

Johnson BD, Hockerman GH, Scheuer T, and Catterall WA (1996) Distinct effects of mutations in transmembrane segment IVS6 on block of L-type calcium channels by structurally similar phenylalkylamines. *Mol Pharmacol* **50:**1388–1400.

Kavanaugh MP, Varnum MD, Osborne PB, Christie MJ, Busch AE, Adelman JP, and North RA (1991) Interaction between tetraethylammonium and amino acid residues in the pore of cloned voltage-dependent potassium channels. *J Biol Chem* **266:**7583–7587.

Kiss L, LoTurco J, and Korn SJ (1999) Contribution of the selectivity filter to inactivation in potassium channels. *Biophys J* **76:**253–263.

Lipkind GM and Fozzard HA (2003) Molecular modeling of interactions of dihydropyridines and phenylalkylamines with the inner pore of the L-type Ca^{2+} channel. *Mol Pharmacol* **63:**499–511.

Liu Y, Jurman ME, and Yellen G (1996) Dynamic rearrangement of the outer mouth of a K^+ channel during gating. *Neuron* **16:**859–867.

Morris GM, Goodsell DS, Halliday RS, Huey R, Hart WE, Belew RK, and Olson AJ (1998) Automated docking using a Lamarckian genetic algorithm and an empirical binding free energy function. *J Comp Chem* **19:**1639–1662.

Morris GM, Goodsell DS, Huey R, and Olson AJ (1996) Distributed automated docking of flexible ligands to proteins: parallel applications of AutoDock 2.4. *J Comput-Aided Mol Des* **10:**293–304.

Nguyen A, Kath JC, Hanson DC, Biggers MS, Canniff PC, Donovan CB, Mather RJ, Bruns MJ, Rauer H, Aiyar J, et al. (1996) Novel nonpeptide agents potently block the C-type inactivated conformation of Kv1.3 and suppress T cell activation. *Mol Pharmacol* **50:**1672–1679.

Panyi G, Sheng Z, and Deutsch C (1995) C-type inactivation of a voltage-gated K^+ channel occurs by a cooperative mechanism. *Biophys J* **69:**896–903.

Peitsch MC (1995) Protein modelling by E-mail. *Bio/Technology* **13:**658–660.

Rauer H and Grissmer S (1996) Evidence for an internal phenylalkylamine action on the voltage-gated potassium channel Kv1.3. *Mol Pharmacol* **50:**1625–1634.

Rauer H and Grissmer S (1999) The effect of deep pore mutations on the action of phenylalkylamines on the Kv1.3 potassium channel. *Br J Pharmacol* **127:**1065–1074.

Röbe RJ and Grissmer S (2000) Block of the lymphocyte K^+ channel mKv1.3 by the phenylalkylamine verapamil: kinetic aspects of block and disruption of accumulation of block by a single point mutation. *Br J Pharmacol* **131:**1275–1284.

Schmalhofer WA, Bao J, McManus OB, Green B, Matyskiela M, Wunderler D, Bugianesi RM, Felix JP, Hanner M, Linde-Arias AR, et al. (2002) Identification of a new class of inhibitors of the voltage-gated potassium channel, Kv1.3, with immunosuppressant properties. *Biochemistry* **41:**7781–7794.

Schmalhofer WA, Slaughter RS, Matyskiela M, Felix JP, Tang YS, Rupprecht K, Kaczorowski GJ, and Garcia ML (2003) Di-substituted cyclohexyl derivatives bind to two identical sites with positive cooperativity on the voltage-gated potassium channel, K(v)1.3. *Biochemistry* **42:**4733–4743.

Schreiber G and Fersht AR (1995) Energetics of protein-protein interactions: analysis of the barnase-barstar interface by single mutations and double mutant cycles. *J Mol Biol* **248:**478–486.

Schuster A, Lacinova L, Klugbauer N, Ito H, Birnbaumer L, and Hofmann F (1996) The IVS6 segment of the L-type calcium channel is critical for the action of dihydropyridines and phenylalkylamines. *EMBO (Eur Mol Biol Organ) J* **15:**2365–2370.

Schwede T, Kopp J, Guex N, and Peitsch MC (2003) SWISS-MODEL: An automated protein homology-modeling server. *Nucleic Acids Res* **31:**3381–3385.

Vennekamp J, Wulff H, Beeton C, Calabresi PA, Grissmer S, Hansel W, and Chandy KG (2004) Kv1.3-blocking 5-phenylalkoxypsoralens: a new class of immunomodulators. *Mol Pharmacol* **65:**1364–1374.

Wrisch A and Grissmer S (2000) Structural differences of bacterial and mammalian K^+ channels. *J Biol Chem* **275:**39345–39353.

Wulff H, Beeton C, and Chandy KG (2003) Potassium channels as therapeutic targets for autoimmune disorders. *Curr Opin Drug Discov Dev* **6:**640–647.

Wulff H, Knaus HG, Pennington M, and Chandy KG (2004) K^+ channel expression during B cell differentiation: implications for immunomodulation and autoimmunity. *J Immunol* **173:**776–786.

Yellen G, Sodickson D, Chen TY, and Jurman ME (1994) An engineered cysteine in the external mouth of a K^+ channel allows inactivation to be modulated by metal binding. *Biophys J* **66:**1068–1075.

Address correspondence to: Stephan Grissmer, Albert-Einstein-Allee 11, 89081 Ulm, Germany. E-mail: stephan.grissmer@uni-ulm.de